# Effects of Inorganic Oxides on Polymer Binder Burnout. I. Poly(vinyl butyral)

**AUROBINDO NAIR and ROBERT L. WHITE***

Department of Chemistry and Biochemistry, University of Oklahoma, Norman, Oklahoma 73019

**SYNOPSIS**

The effects of silica, mullite, $\alpha$-alumina, and $\gamma$-alumina on the nonoxidative thermal degradation of poly(vinyl butyral) are described. To varying degrees, all of the inorganic oxides catalyzed reactions that produced butanal. Other significant products included: water, butenal, acetic acid, and alkyl aromatics. Two distinct evolution steps were detected for samples containing mullite and $\alpha$-alumina, suggesting that multiple interactions existed between these oxides and the polymer. The relative amounts of volatile aromatic products evolved by heating polymer/oxide samples were greater than the amounts generated from the neat polymer. For the polymer/$\gamma$-alumina sample, carboxylate species were detected on oxide surfaces above 250°C, indicating that a reaction between the polymer and $\gamma$-alumina occurred. © 1996 John Wiley & Sons, Inc.

## INTRODUCTION

Polymers are used in the manufacturing of ceramics to hold inorganic oxide powders in place prior to sintering.[1-7] The process of polymer thermal decomposition that occurs during ceramic product manufacturing is known as binder burnout. Ideally, polymer binders should decompose completely during the early stages of sintering. Although complete polymer decomposition can usually be achieved in oxidative sintering atmospheres, incomplete binder burnout can often occur in the inert or reductive atmospheres that are required for fabricating ceramic substrates for use in the microelectronics industry.

Poly(vinyl butyral) (PVB) is commonly used as a ceramic binder for nonoxidative ceramic sintering. Commercial grade PVB is manufactured by converting poly(vinyl acetate) to poly(vinyl alcohol) and then reacting this polymer with butanal. This process does not lead to complete conversion to poly(vinyl butyral), but, instead, results in a multifunctional polymer containing residual acetate and hydroxyl groups:

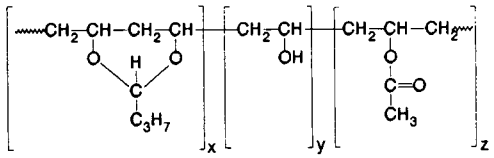

The composition of commercial grade PVB is typically: x > 75%, y = 18–22%, and z < 3%.

PVB adheres to inorganic oxides through interactions between oxide surfaces and polymer hydroxyl groups.[8,9] In addition, the carbonyl oxygens of acetate groups present in PVB can interact with oxide surfaces through hydrogen bonding with surface hydroxyls.[10] Neat PVB thermal decomposition occurs predominantly by an intramolecular elimination mechanism:[11]

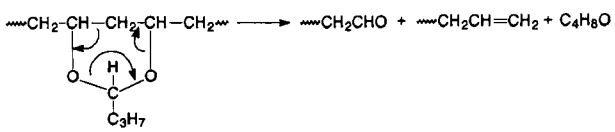

This process yields butanal and results in the formation of unsaturated and aldehyde polymer chain ends. Because commercial grade PVB contains a large fraction of hydroxyl groups and some acetate functionalities, a significant fraction of thermal degradation products arise from reactions that do not involve butyral functionalities. For example, re-

* To whom correspondence should be addressed.

Journal of Applied Polymer Science, Vol. 60, 1901–1909 (1996)
 CCC 0021-8995/96/111901-09

moval of hydroxyl groups via dehydration is an important PVB thermal degradation process:[12,13]

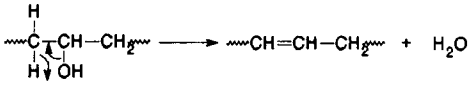

The thermal degradation of vinyl alcohol polymer segments can also result in the formation of $CH_3(CH{=}CH)_nCHO$ and $CH_3(CH{=}CH)_nCOCH_3$ homologs by free radical hydrogen abstractions:[12,14]

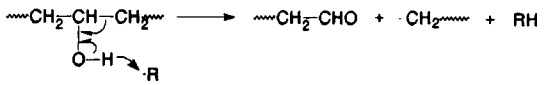

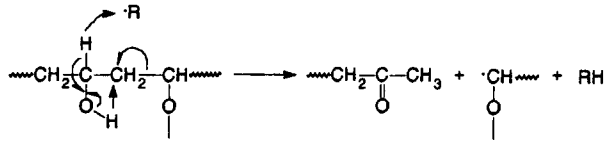

In addition, the thermal degradation of PVB acetate functionalities can result in production of acetic acid:[15,16]

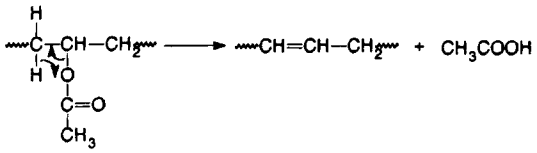

It is known that inorganic oxides can interact with polymer binders during binder burnout and that these interactions affect polymer thermal degradation processes.[13,17-22] If significant quantities of polymer residue remain above temperatures at which ceramic sintering begins, flaws in ceramic end products may result. It is, therefore, useful to examine the effects of inorganic oxides on the nonoxidative thermal degradation of polymer binders used in electronics industry applications. The effects of silica, mullite, $\alpha$-alumina, and $\gamma$-alumina on the thermal decomposition of PVB are described here.

## EXPERIMENTAL

### Apparatus

Pyrolysis–GC/MS experiments were performed by using a microfurnace pyrolysis injector built in our laboratory and described elsewhere.[23] Separations were achieved by using a Hewlett Packard (Palo Alto, CA) capillary gas chromatograph equipped with a 30 m × 0.25 mm i.d. Hewlett Packard HP-1 column (0.52 $\mu$m crosslinked methyl silicone film thickness) in series with a 30 m × 0.32 mm i.d. Alltech (Deerfield, IL) Econo-Cap column (0.25 $\mu$m carbowax film thickness). The gas chromatograph oven temperature program consisted of a 1 min isothermal period at 70°C followed by a 2°C/min ramp to 90°C, a 20°C/min ramp to 250°C, and a 10 min isothermal period at 250°C. The He carrier gas flow rate was maintained at 2 mL/min during separations. Mass spectra were acquired by a Hewlett Packard 5988 quadrupole mass spectrometer scanning from m/z 10 to 250 at a rate of 20 spectra/min. Mass spectral library searches employed a 36,218 spectra NBS mass spectral library.

Thermogravimetry–mass spectrometry (TG–MS) measurements were made by connecting the gas outlet of a Du Pont (Wilmington, DE) Model 951 thermogravimetric analyzer (TGA) to a Hewlett Packard 5985 quadrupole mass spectrometer by using a Scientific Glass Engineering Inc. (Austin, TX) MCVT-1–50 variable splitting valve. The TG–MS interface was maintained at 200°C during measurements. Helium flow through the TGA during measurements was maintained at a rate of 50 mL/min. Polymer/oxide samples were heated from 50°C to 600°C at nominal rates of 5, 10, 25, and 50°C/min. Mass spectra were acquired by using 70 eV electron bombardment ionization and scanning from m/z 10 to m/z 500 at a rate sufficient to record at least one signal-averaged spectrum for each 4°C temperature increment. The mass spectrometer ion source pressure was maintained at $2 \times 10^{-5}$ torr during TG–MS analyses.

The variable temperature diffuse reflectance infrared spectroscopy (VT-DRIFTS) apparatus used in this study and procedures for acquiring VT-DRIFTS spectra have been described previously.[24-28] About 15 mg quantities of samples were placed in the sample holder for measurements. The DRIFTS sample chamber He purge gas flow rate was maintained at 10 mL/min during VT-DRIFTS measurements. A heating rate of 10°C/min from 50 to 600°C was used for VT-DRIFTS measurements. DRIFTS measurements were made at a rate of 1 spectrum/min over the 4000 to 750 $cm^{-1}$ range at a spectral resolution of 8 $cm^{-1}$.

### Samples

Silica, mullite, and commercial grade PVB (MW $1.5–3.0 \times 10^5$) were obtained from Hitachi (Hitachi City, Japan), $\alpha$-alumina was purchased from Aldrich Chemical Co. (Milwaukee, WI), $\gamma$-alumina was pur-

**Table I Inorganic Oxide Surface Areas**

| Oxide | Hydroxyl Content % $H_2O$ (wt/wt) | Surface Area ($m^2/g$) |
|---|---|---|
| Silica | 0.59 | 10.96 ± 1.19 |
| Mullite | 0.48 | 2.14 ± 0.36 |
| $\alpha$-Alumina | 0.33 | 0.68 ± 0.05 |
| $\gamma$-Alumina | 6.37 | 96.72 ± 8.22 |

chased from Johnson Matthey/AESAR (Seabrook, NH), and 1-butanol was purchased from Sigma Chemical Co. (St. Louis, MO). Helium (99.9995%) was purchased from Union Carbide Corp., Linde Division (Danbury, CT). Inorganic oxides were sieved prior to polymer/oxide sample preparation to restrict particle sizes to 63–150 $\mu$m. Inorganic oxide surface areas and hydroxyl contents represented as weight percent water are given in Table I. Surface areas were measured by using a Micromeritics Instrument Corp. (Norcross, GA) FlowSorb II 2300 surface area analyzer and hydroxyl contents were measured by TG–MS. Approximately 10% (wt/wt) PVB/oxide samples were prepared by dissolving 1.7 g of PVB in 250 mL of 1-butanol, adding 25 mL of this solution to 1.5 g of oxide, and rotoevaporating the mixture to remove the solvent.

## RESULTS

Pyr-GC/MS was employed to generate and identify thermal degradation products formed by rapidly heating PVB/oxide samples to 500°C. The relative amounts of degradation products evolved from neat PVB and the PVB/oxide samples are listed in Table II. Compared to neat PVB, the amounts of butanal evolved from the PVB/oxide samples were slightly lower. Significant amounts of CO and $CO_2$ were evolved from all samples, although the relative amount evolved from the PVB/$\gamma$-alumina sample was considerably less than the other samples. The larger fraction of water generated from the PVB/$\gamma$-alumina sample was consistent with the fact that $\gamma$-alumina contained substantially more hydroxyl groups than the other oxides (Table I). Compared to the neat polymer, more volatile aromatic species were generated from the PVB/oxide samples. The PVB/$\alpha$-alumina and PVB/$\gamma$-alumina samples produced larger amounts of butenal than the neat PVB, PVB/silica, and PVB/mullite samples. Table II also shows that the relative amounts of acetic acid generated from the PVB/$\alpha$-alumina and PVB/$\gamma$-alumina samples were less than the amounts produced from the other samples.

By using TG–MS, the thermal decomposition processes for neat PVB were studied under conditions that were similar to those employed for nonoxidative ceramic sintering. Figure 1 shows the weight loss curve and species-specific ion signal temperature profiles obtained by TG–MS analysis of neat PVB. Species-specific ions were selected after comparing the mass spectra of the primary volatile products detected by pyr-GC/MS analysis of the PVB and PVB/oxide samples to find ions that were unique to specific volatile products. The ions monitored and the species that they represented were: m/z 18 (water), m/z 60 (acetic acid), m/z 70 (butenal), m/z 72 (butanal), and m/z 91 (alkyl aromatics). PVB weight loss began to occur at approximately 350°C and was complete at about 450°C. The temperatures corresponding to peak maxima ($T_M$) were near 400°C for ions representing aliphatic species and near 410°C for alkyl aromatics.

**Table II Neat PVB and PVB/Oxide pyr-GC/MS Products at 500°C**

| Product | Oxide | | | | |
|---|---|---|---|---|---|
| | Neat PVB | Silica | Mullite | $\alpha$-Alumina | $\gamma$-Alumina |
| CO, $CO_2$ | 10.2[a] | 9.6 | 10.4 | 13.8 | 5.6 |
| Acetaldehyde | 4.5 | 2.5 | 3.8 | 7.6 | 4.3 |
| Acetone | 1.0 | 2.2 | 2.2 | 1.6 | 1.6 |
| Butanal | 60.8 | 57.7 | 56.0 | 52.8 | 55.6 |
| $H_2O$ | 1.1 | 2.5 | 2.2 | 1.0 | 6.9 |
| Benzene | 1.2 | 1.2 | 2.1 | 0.9 | 3.3 |
| Alkyl Aromatics | 0.1 | 0.5 | 0.1 | 0.7 | 0.3 |
| Butenal | 9.3 | 9.2 | 7.3 | 14.1 | 16.6 |
| Acetic Acid | 2.9 | 3.1 | 2.9 | 1.4 | 1.7 |

[a] Percentage of integrated total ion current.

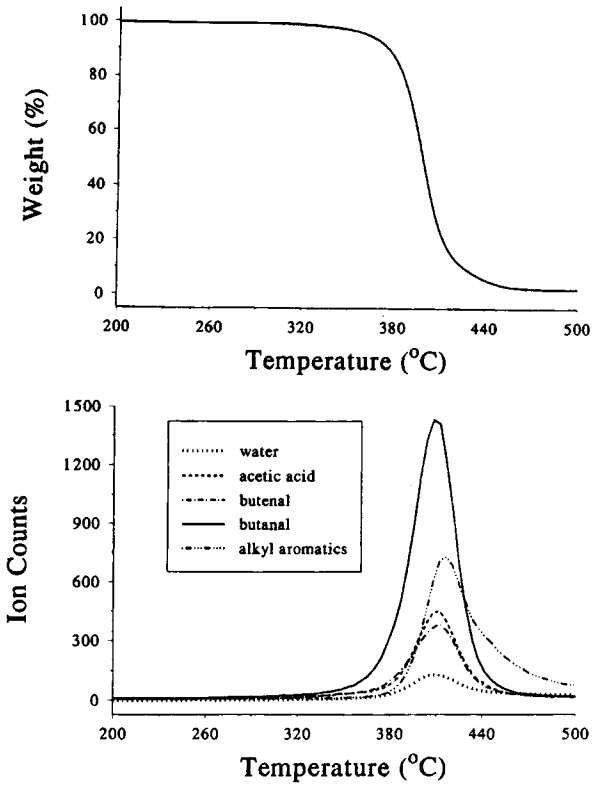


**Figure 1** Weight loss curve and ion signal temperature profiles obtained by TG–MS analysis of neat PVB.

PVB-coated inorganic oxide samples were also analyzed by TG–MS. Figure 2 shows the weight loss curve and species-specific ion signal temperature profiles for a PVB/silica sample obtained by TG–MS analysis. Like neat PVB, significant weight loss for the PVB/silica sample began at approximately 350°C. However, sample weight loss was complete at about 480°C, which was about 30°C higher than the corresponding temperature for neat PVB. The maxima of the ion signal temperature profiles representing volatile aliphatic species occurred at about 395°C, which was about the same temperature as was measured for the same species during neat PVB degradation. The ion signal temperature profile for alkyl aromatics comprised two overlapping peaks with maxima at about 407 and 450°C.

Figure 3 shows the weight loss curve and species-specific ion signal temperature profiles for a PVB/mullite sample. Weight loss for the PVB/mullite sample began at approximately 300°C and was complete at about 475°C. The weight loss onset temperature for this sample was approximately 50°C lower than those measured for neat PVB and the PVB/silica sample. The temperature profiles for ions representing volatile aliphatic species comprised two overlapping asymmetric peaks with maxima at about 335 and 350°C. Unlike the other ion profiles, the ion signal temperature profile for alkyl aromatics consisted of three overlapping peaks. Two of these peaks coincided with those for the other ion signals profiled. The third peak maximized at about 435°C.

Figure 4 shows the weight loss curve and species-specific ion signal temperature profiles for a PVB/$\alpha$-alumina sample. Weight loss for the PVB/$\alpha$-alumina sample began at approximately 300°C and was complete at about 450°C. Although the PVB/$\alpha$-alumina sample weight loss onset temperature was similar to that for the PVB/mullite sample, weight loss for this sample was complete at approximately 25°C lower temperature. The temperature profiles for ion signals representing volatile aliphatic species comprised two overlapping asymmetric peaks with maxima at about 340 and 390°C. With the exception of butenal, the peak detected at higher temperature was larger. Both peaks were of approximately equal magnitude in the butenal ion signal temperature profile. Two overlapping peaks were also detected in the ion signal profile representing alkyl aromatics. The first of these peaks maximized near 400°C, and the second peak maximum occurred at about 450°C.

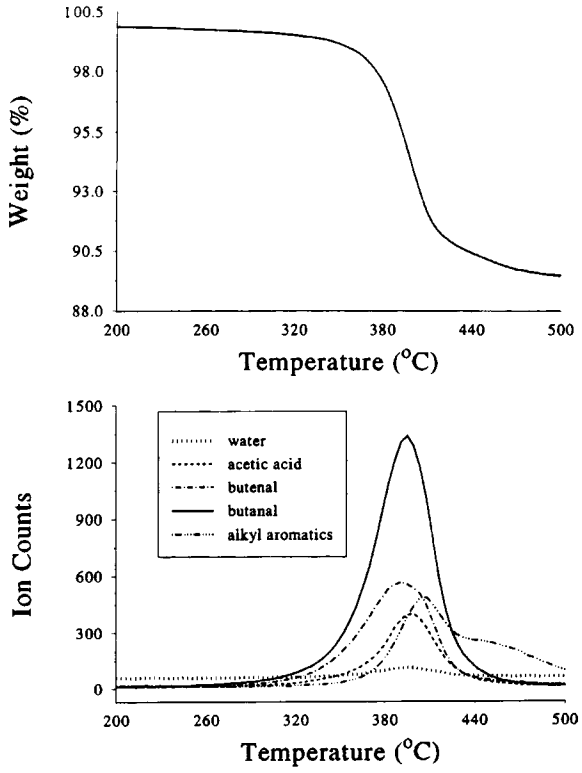


**Figure 2** Weight loss curve and ion signal temperature profiles obtained by TG–MS analysis of a PVB/silica sample.

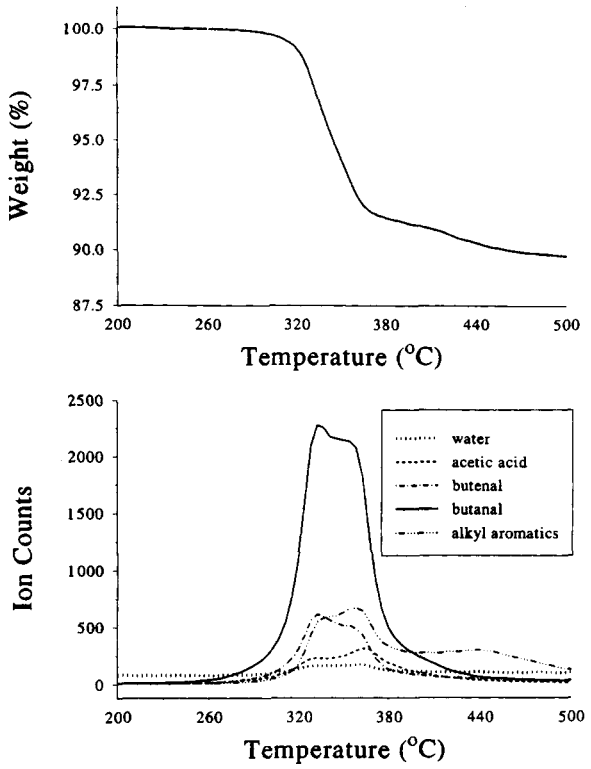


**Figure 3** Weight loss curve and ion signal temperature profiles obtained by TG–MS analysis of a PVB/mullite sample.

Figure 5 shows the weight loss curve and species-specific ion signal temperature profiles for a PVB/$\gamma$-alumina sample. Weight loss for the PVB/$\gamma$-alumina sample began immediately upon sample heating and continued throughout the TG–MS temperature range. The most significant weight loss occurred at 200–350°C. In contrast to the other samples, no acetic acid was detected during TG–MS analysis of the PVB/$\gamma$-alumina sample. The ion signal attributed to water was large over the entire temperature range and was similar to that detected by TG–MS analysis of neat $\gamma$-alumina. The ion signal temperature profiles for butanal, butenal, and acetone were broad peaks centered at about 285°C, which was approximately 115°C lower than the peak maxima for the same ions detected by TG–MS analysis of neat PVB. The ion signal temperature profile representing alkyl aromatics comprised two overlapping asymmetric peaks with maxima at about 300 and 420°C.

VT-DRIFTS was employed to examine functional group changes in the polymer residue that occurred during thermal degradation of PVB/oxide samples. The O—H stretching vibration band observed in DRIFTS infrared spectra was due to PVB hydroxyls, oxide hydroxyls, and adsorbed water, whereas the C—H stretching vibration band was representative of the polymer only. Figure 6(a) shows the integrated absorbance temperature profiles for O—H stretching vibrations (3800–3050 $cm^{-1}$) and C—H stretching vibrations (3030–2765 $cm^{-1}$) during decomposition of the PVB/silica sample. Hydroxyl loss began immediately upon sample heating and continued linearly up to 500°C. Significant absorbance decreases in the C—H spectral region occurred only above 400°C. Figure 6(b) shows the integrated absorbance temperature profiles representing O—H and C—H functionalities during the PVB/mullite sample decomposition. Hydroxyl loss began immediately upon sample heating and continued linearly until about 300°C, at which temperature the rate of hydroxyl loss increased. Above 350°C, the rate of hydroxyl loss decreased substantially. Significant absorbance decreases in the C—H spectral region occurred as two steps above 300°C, with the second step beginning at about 375°C. Figure 6(c) shows the integrated absorbance temperature profiles representing O—H and C—H functionalities during the PVB/$\alpha$-alumina sample de-

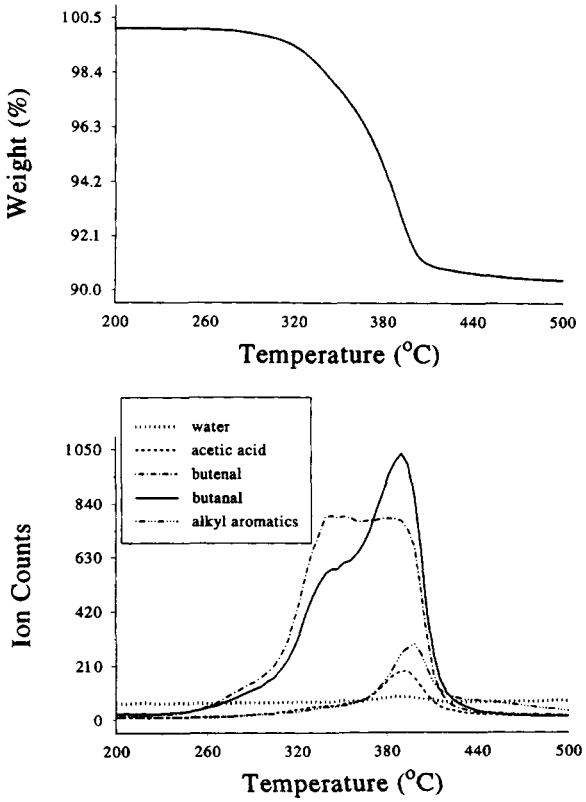


**Figure 4** Weight loss curve and ion signal temperature profiles obtained by TG–MS analysis of a PVB/$\alpha$-alumina sample.

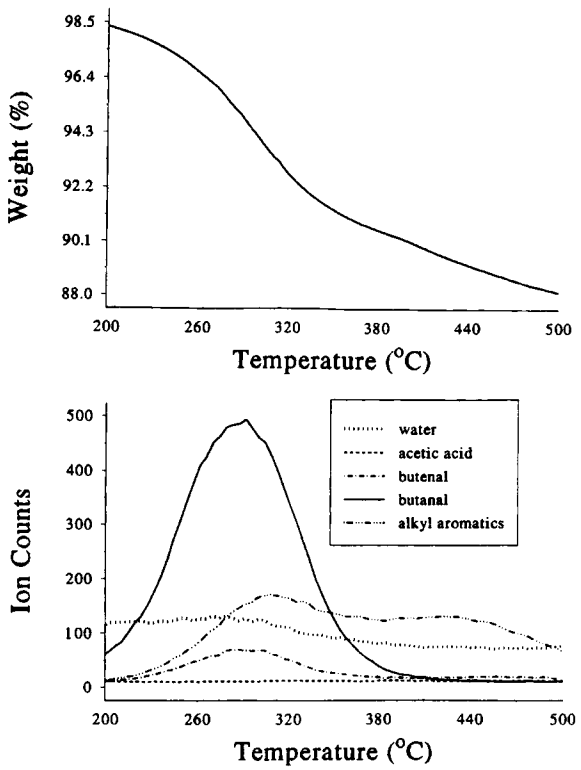


**Figure 5** Weight loss curve and ion signal temperature profiles obtained by TG–MS analysis of a PVB/$\gamma$-alumina sample.

composition. Hydroxyl loss for the PVB/$\alpha$-alumina sample occurred in two steps. The first step began immediately after the start of the heating ramp and continued linearly up to about 350°C. At this temperature, the rate of hydroxyl loss increased. Loss of hydroxyl absorbance was complete at about 390°C. Like the PVB/mullite sample, significant absorbance decreases in the C—H spectral region were detected for the PVB/$\alpha$-alumina sample above 300°C in two steps, with the second step beginning at about 400°C. Figure 6(d) shows the integrated absorbance temperature profiles representing O—H and C—H functionalities during PVB/$\gamma$-alumina decomposition. Like the other PVB/oxide samples, hydroxyl loss began immediately upon sample heating. The steepest rate of hydroxyl loss occurred between 200 and 300°C. A significant decrease in the C—H stretching vibration absorbance began at about 250°C. Unlike the other PVB/oxide samples, a band at 1575 $cm^{-1}$ appeared in the PVB/$\gamma$-alumina sample infrared spectra above 250°C. The 1575 $cm^{-1}$ band intensity temperature profile derived from VT-DRIFTS spectra is shown in Figure 7. This band, which was attributed to carboxylate formation,[22,29] appeared in infrared spectra near 200°C and diminished in intensity above 450°C.

Water vapor is often added to nonoxidative sintering atmospheres to utilize the water gas reaction to remove carbon that forms during binder burnout. For the TG–MS analysis conditions employed here, temperatures must exceed 900°C before the effects of the water gas reaction become evident.[21] However, to ascertain the effects of water vapor on PVB binder burnout processes that occurred below 900°C, the previously described TG–MS experiments were repeated while purging samples with helium that had been saturated with water vapor. TG–MS results obtained in this manner were found to be indistinguishable from those derived from measurements for which dry helium was employed for sample purging.

## DISCUSSION

Pyr-GC/MS results (Table II) showed that the amounts of volatile alkyl aromatics produced by heating PVB/oxide samples were greater than the amounts produced from neat PVB. TG–MS ion signal temperature profiles (Figs. 2 to 5) indicated that evolution of aromatics continued well above temperatures at which the primary degradation products were generated. This was expected because these species were likely produced from polyene segments in the polymer residue that were formed only after significant polymer decomposition. The second steps in VT-DRIFTS C—H stretching vibration integrated absorbance profiles for the PVB/mullite and PVB/$\alpha$-alumina samples occurred within the temperature range over which alkyl aromatics were detected by TG–MS and were probably representative of aromatic species evolution. Although this second step was not obvious in VT-DRIFTS temperature profiles for neat PVB and the PVB/silica and PVB/$\gamma$-alumina samples, TG–MS ion signal temperature profiles confirmed that aromatics were evolved at temperatures above those at which the primary polymer decomposition processes occurred. In addition, small olefinic C—H stretching vibration absorbance bands were detected near 3050 $cm^{-1}$ in VT-DRIFTS spectra acquired above 400°C for the PVB/$\alpha$-alumina and PVB/$\gamma$-alumina samples.

The onset temperatures for the decrease in the C—H stretching vibration absorbance for the PVB/oxide samples exhibited trends consistent with those observed for the TG–MS weight loss curves. For example, the temperature corresponding to weight loss onset was lowest for the PVB/$\gamma$-alumina sample

(ca. 200°C), which also exhibited the lowest onset temperature for C—H absorbance decrease (ca. 200°C). The PVB/silica sample weight loss onset temperature was the highest among the PVB/oxides (ca. 380°C), and this sample also had the highest onset temperature for C—H absorbance decrease (ca. 400°C). The weight loss onset temperatures for the PVB/$\alpha$-alumina and PVB/mullite samples were at about 300°C, which was about the same temperature that the onset of C—H absorbance decrease was detected for these samples.

Pyr-GC/MS and TG-MS analysis indicated that reactions that produced butanal were responsible for most of the PVB/oxide sample weight losses. This was expected because poly(vinyl butyral) moieties comprised more than 75% of the PVB polymer used in this study. Ion signal temperature profiles derived from TG–MS analyses of the PVB/mullite and PVB/$\alpha$-alumina samples exhibited two overlapping peaks for the most prominent volatile products, suggesting that mullite and $\alpha$-alumina surfaces were capable of multiple interactions with PVB functionalities. Pyr-GC/MS and TG–MS results also indicated that butenal was produced in significant quantities from PVB and PVB/oxide samples. Bu-

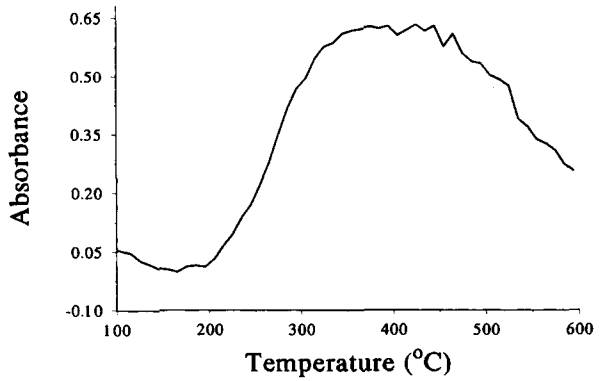


**Figure 7** The 1575 $cm^{-1}$ carboxylate band intensity temperature profile obtained by VT-DRIFTS analysis of a PVB/$\gamma$-alumina sample.

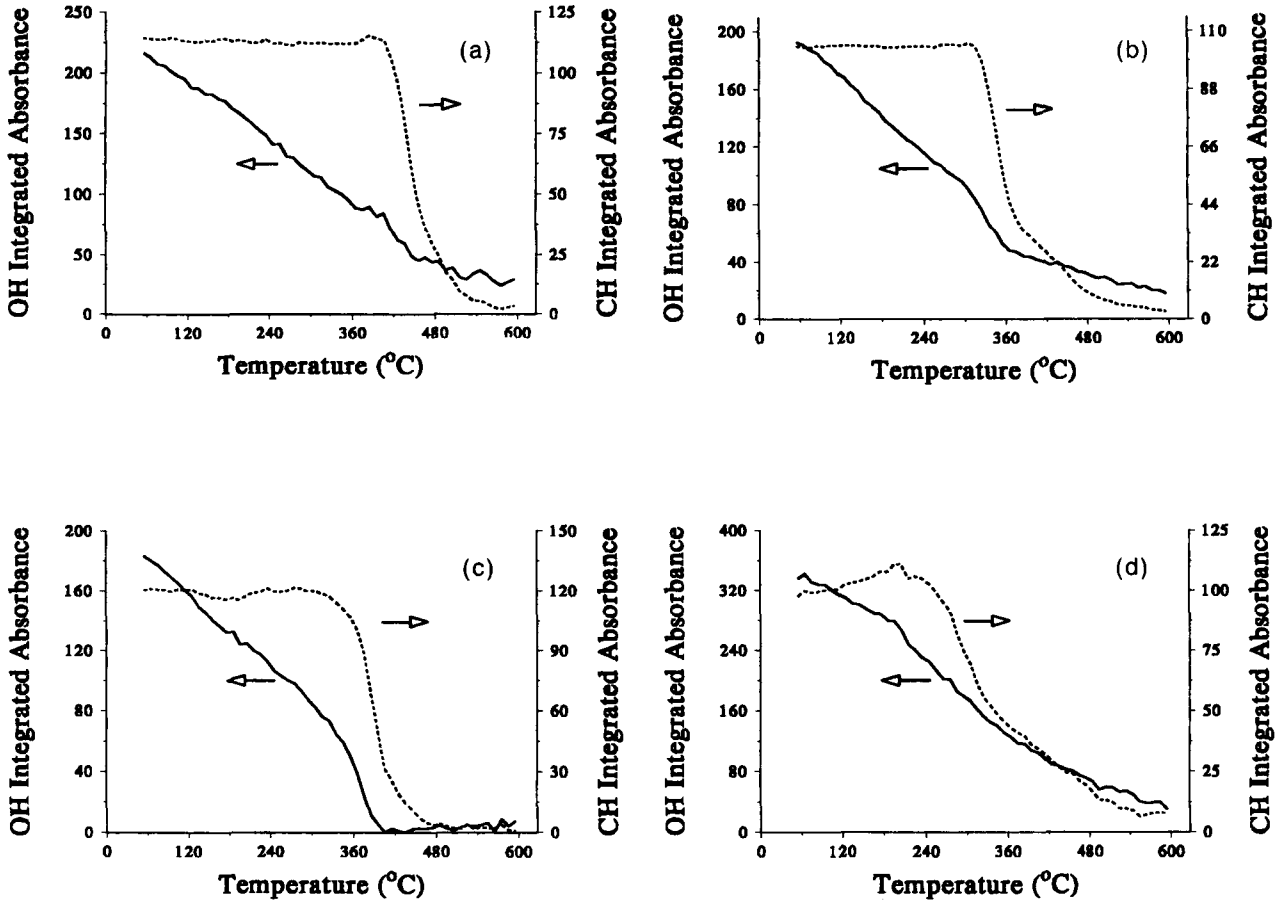


**Figure 6** OH (3800–3050 $cm^{-1}$) and CH (3030–2765 $cm^{-1}$) integrated absorbance temperature profiles obtained by VT-DRIFTS analysis of (a) PVB/silica, (b) PVB/mullite, (c) PVB/$\alpha$-alumina, and (d) PVB/$\gamma$-alumina samples.

**Table III Kinetic Parameters for Butanal Evolution from Neat PVB and PVB/Oxides**

| Neat PVB or PVB/Oxide | $T_M$ (°C) | $E_a$ (kcal mol$^{-1}$) | A ($s^{-1}$) |
|---|---|---|---|
| Neat PVB | 398 | 44.5 ± 0.6 | $2.9 \times 10^{12} \pm 7.7 \times 10^{10}$ |
| Silica | 395 | 42.8 ± 0.2 | $8.6 \times 10^{11} \pm 5.0 \times 10^{9}$ |
| Mullite | 343 | 23.4 ± 1.9 | $1.5 \times 10^{6} \pm 1.7 \times 10^{5}$ |
| $\alpha$-Alumina | 390 | 36.5 ± 3.1 | $8.1 \times 10^{9} \pm 9.7 \times 10^{8}$ |
| $\gamma$-Alumina | 287 | 30.5 ± 1.9 | $6.7 \times 10^{9} \pm 6.0 \times 10^{8}$ |

tenal can be formed by intramolecular butanal eliminations from poly(vinyl butyral) segments adjacent to unsaturated or aldehyde polymer chain ends that were created by a previous intramolecular butanal elimination. Depending on which poly(vinyl butyral) segment oxygen atom was ultimately incorporated into the butanal molecule, 1,3-propane dialdehyde and 1,4-pentadiene could also be produced by this elimination pathway. However, neither of these substances were detected in significant quantities by pyr-GC/MS. Alternatively, 3-butenal might be formed by a polymer unzipping mechanism that would also yield butanal:[30]

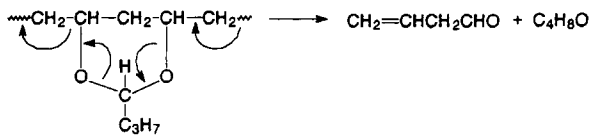


The fact that the quantities of butenal detected by pyr-GC/MS analysis of the PVB and PVB/oxide samples were significantly less than the amounts of butanal (Table II) suggests that an unzipping mechanism that yielded equimolar amounts of butanal and 3-butenal was not the primary pathway for butanal formation. The variability in the amounts of butenal detected by pyr-GC/MS analysis of the PVB/oxide samples and the fact that samples containing $\alpha$-alumina and $\gamma$-alumina generated significantly more butenal than the other oxides suggests that interactions between PVB and inorganic oxides altered which PVB thermal degradation pathways were favored when samples were heated at rates similar to those employed for ceramic sintering. For example, TG–MS analysis of the PVB/$\alpha$-alumina sample (Fig. 4) revealed that the relative amount of butenal produced by heating this sample at 10°C/min to 350°C was greater than the amounts produced from heating the other polymer/oxide samples. In fact, between 250 and 360°C, the TG–MS butenal molecular ion (m/z 70) signal was greater than the butanal molecular ion (m/z 72) signal for this sample.

Thermal degradation of residual alcohol moieties in PVB resulted in the evolution of water and acetone, whereas decomposition of residual acetate functionalities resulted in the evolution of acetic acid. Ion signal temperature profiles for these species were somewhat different from the butanal specific ion profiles, confirming that the formation of these species involved different mechanisms. The appearance of a carboxylate absorbance band in VT-DRIFTS spectra and the lack of acetic acid evolution from the PVB/$\gamma$-alumina sample suggested that acetic acid formed by polymer decomposition reacted with the $\gamma$-alumina surface to form carboxylate. Although carboxylate was not detected in the PVB/$\alpha$-alumina sample infrared spectra, significantly less acetic acid was evolved from this sample compared to neat PVB during pyr-GC/MS analysis, suggesting that, like the PVB/$\gamma$-alumina sample, acetic acid evolved from acetate group decomposition reacted with the oxide surface.

Table III contains m/z 72 ion signal temperature profile $T_M$ values derived from TG–MS mass spectra obtained by heating samples at 10°C/min and kinetic parameters representing the evolution of butanal. Apparent activation energies and frequency factors were calculated for each PVB/oxide sample from TG–MS mass spectral data by using the method described by Risby and Yergey.[31] When multiple butanal evolution peaks were detected, kinetic parameters were calculated based on the most intense peak in the ion signal temperature profile. Table III shows that silica had little effect on butanal formation and that the other oxides catalyzed these reactions. Activation energies and frequency factors for samples comprised of PVB coated on mullite, $\alpha$-alumina, and $\gamma$-alumina were significantly lower than those for neat PVB and the PVB/silica sample. For the PVB/$\alpha$-alumina sample, the effect of a lower activation energy relative to that calculated for neat PVB was virtually offset by a significantly lower frequency factor, resulting in a $T_M$ value that was only slightly different from that for neat PVB. Offsetting changes in kinetic parameters are commonly

observed when the same reaction is carried out under different environmental conditions.[32] Although the butanal evolution activation energy for the PVB/mullite sample was lower than that for the PVB/$\gamma$-alumina sample, the significantly lower frequency factor for this sample caused the $T_M$ value for the PVB/mullite sample to be greater than that for the PVB/$\gamma$-alumina sample.

## CONCLUSIONS

PVB thermal degradation was catalyzed by all of the oxides. As a result, the weight loss onset temperatures for the PVB/oxide samples were lower than the corresponding temperature measured for neat PVB. However, the specific effects of the oxides on the PVB thermal degradation pathways were different. Although PVB began to decompose at lower temperatures when oxides were present, significantly more alkyl aromatics were evolved from PVB/oxide samples than from neat PVB. TG–MS results indicated that alkyl aromatic evolution was enhanced when mullite, $\alpha$-alumina, and $\gamma$-alumina were present, suggesting that oxide surface polarity may be a factor in determining the relative importance of this reaction pathway. Aromatization is not a desired binder burnout process because it indicates that carbonization may be occurring on oxide surfaces, which can lead to flaws in ceramic products.

Financial support for this work from Hitachi, Ltd. is gratefully acknowledged.

## REFERENCES

1. R. A. Gardner and R. W. Nufer, *Solid State Technol.*, **17,** 38 (1974).
2. F. Aldinger and H. J. Kalz, *Angew. Chem. Int. Ed. Engl.*, **26,** 371 (1987).
3. G. Petzow, *Pract. Met.*, **25,** 53 (1988).
4. J. Semen and J. G. Loop, *Ceram. Eng. Sci. Proc.*, **11,** 1387 (1990).
5. F. Aldinger, H. Cherdron, K. Kuhlein, and J. Riggs, *Adv. Mater.*, **4,** 138 (1992).
6. J. Bohnlein-Mauss, W. Sigmund, G. Wegner, W. H. Meyer, F. Hessel, K, Seitz, and A. Roosen, *Adv. Mater.*, **4,** 73 (1992).
7. S. M. Johnson, Y. D. Blum, G. A. McDermott, and M. I. Gusman, *Scripta Metallurg. Mater.*, **31,** 1025 (1994).
8. K. Nakamae, K. Sumiya, T. Taii, and T. Matsumoto, *J. Polym. Sci., Polym. Symp.*, **71,** 109 (1984).
9. M. D. Sacks and G. W. Scheiffele, *Adv. Ceram.*, **19,** 175 (1986).
10. K. E. Howard, C. D. E. Lakeman, and D. A. Payne, *J. Am. Ceram. Soc.*, **73,** 2543 (1990).
11. F. Bakht, *Pakistan J. Sci. Ind. Res.*, **26,** 35 (1983).
12. G. Montaudo, C. Publisi, E. Scamporrino, and D. Vitalini, *J. Polym. Sci., Polym. Chem. Ed.*, **24,** 301 (1986).
13. R. L. White and A. Nair, *Chem. Mater.*, **2,** 742 (1990).
14. J. G. Pritchard, *Poly(vinyl alcohol) Basic Properties and Uses,* Gordon and Breach Science Publishers, New York, 1970, p. 81.
15. N. Grassie, *Trans. Faraday Soc.*, **48,** 379 (1952).
16. A. Ballisteri, S. Foti, G. Montauelo, and E. Scamporrino, *J. Polym. Sci., Polym. Chem. Ed.*, **18,** 1147 (1980).
17. M. J. Cima and J. A. Lewis, *Ceram. Trans.*, **1,** 567 (1988).
18. Y. N. Sun, M. D. Sacks, and J. W. Williams, *Ceram. Trans.*, **1,** 538 (1988).
19. M. J. Cima, J. A. Lewis, and A. D. Devoe, *J. Am. Ceram. Soc.*, **72,** 1192 (1989).
20. S. Masia, P. D. Calvert, W. E. Rhine, and H. K. Bowen, *J. Mater. Sci.*, **24,** 1907 (1989).
21. R. L. White and J. Ai, *Chem. Mater.*, **4,** 233 (1992).
22. J. Ai, L. L. Phegley, G. Christen, and R. L. White, *J. Am. Ceram. Soc.*, **78,** 874 (1995).
23. R. L. White, *J. Anal. Appl. Pyr.*, **18,** 269 (1991).
24. R. L. White, *J. Anal. Appl. Pyr.*, **18,** 325 (1991).
25. R. L. White, *Appl. Spectrosc.*, **46,** 1508 (1992).
26. R. L. White, *Anal. Chem.*, **64,** 2010 (1992).
27. R. L. White, *Appl. Spectrosc.*, **47,** 1492 (1993).
28. R. Lin and R. L. White, *Anal. Chem.*, **66,** 2976 (1994).
29. Y. N. Sun, M. D. Sacks, and J. W. Williams, *Ceram. Trans.*, **1,** 538 (1988).
30. G. C. Kingston and H. K. Yuen, *Thermochim. Acta,* **116,** 317 (1987).
31. T. H. Risby and A. L. Yergey, *Anal. Chem.*, **50,** 326A (1978).
32. C. N. Hinshelwood, *Angew. Chem.*, **69,** 445 (1957).

*Received August 10, 1995*
*Accepted December 6, 1995*